



Global atmospheric ethane, propane and methane trends (2006-2016)

Mengze Li ¹, Andrea Pozzer ¹, Jos Lelieveld ¹, Jonathan Williams ¹

¹ Max Planck Institute for Chemistry, Hahn-Meitner-Weg 1, 55128 Mainz, Germany

5 *Correspondence to:* Jonathan Williams (jonathan.williams@mpic.de); Andrea Pozzer (andrea.pozzer@mpic.de);
Mengze Li (mengze.li@mpic.de)

Abstract. Methane, ethane and propane are among the most abundant hydrocarbons in the atmosphere. These compounds have many emission sources in common and are all primarily removed through OH oxidation. Their mixing ratios and long-term trends in the upper troposphere and stratosphere are rarely reported due to the paucity of measurements. In this study, we present long-term (2006-2016) global ethane, propane, and methane data from airborne observation in the Upper Troposphere - Lower Stratosphere (UTLS) region, combined with atmospheric model simulations for ethane at the same times and locations, to focus on global ethane trends. The model uses the Copernicus emission inventory CAMS-GLOB and distinguishes 12 ethane emission sectors (natural and anthropogenic): BIO (biogenic emission), BIB (biomass burning), AWB (agricultural waste burning), ENE (power generation), FEF (fugitives), IND (industrial processes), RES (residential energy use), SHP (ships), SLV (solvents), SWD (solid waste and waste water), TNR (off-road transportation), and TRO (road transportation). The results from the model simulations were compared with observational data and further optimized. The Northern Hemispheric (NH) upper tropospheric and stratospheric ethane trends were $0.33 \pm 0.27\%/yr$ and $-3.6 \pm 0.3\%/yr$, respectively, in 2006-2016. The global ethane emission for this decade was estimated to be 19.28 Tg/yr. Trends of methane and propane, and of the 12 model sectors provided more insights on the variation of ethane trends. FEF, RES, TRO, SWD and BIB are the top five contributing sectors to the observed ethane trends. An ethane plume for NH upper troposphere and stratosphere in 2010-2011 was identified to be due to fossil fuel related emissions, likely from oil and gas exploitation. The discrepancy between model results and observations suggests that the current ethane emission inventories must be improved and higher temporal-spatial resolution data of ethane are needed. This dataset is of value to future global ethane budget estimates and the optimization of current ethane inventories. The data are public accessible at <https://doi.org/10.5281/zenodo.5112059> (Li et al., 2021b).



1. Introduction

Ethane (C_2H_6) is among the most abundant non-methane hydrocarbons (NMHC) present in the atmosphere. Major sources of ethane to the atmosphere are via natural gas and oil production (~62%), biofuel combustion (20%) and biomass burning (18%). Interestingly 84% of its total emissions are from the Northern Hemisphere (NH) (Xiao et al., 2008). Oxidation by hydroxyl (OH) radicals is the major atmospheric loss process for tropospheric ethane while in the stratosphere the reaction with chlorine (Cl) radicals provides an additional loss processes (Li et al., 2018). Due to the seasonal variation of ethane emissions and the photochemically generated OH radicals, ethane has a clear annual cycle in concentration, showing higher levels in winter. Its global lifetime is circa three months, with a minimum in summer (~2 months) and a maximum in winter (~10 months) (Helmig et al., 2016; Li et al., 2018; Xiao et al., 2008). Ethane oxidation forms acetaldehyde, which in turn contributes to the formation of PAN (peroxyacetyl nitrate) or peracetic acid depending on the levels of NO_x (Millet et al., 2010). PAN acts as a reservoir species of nitrogen oxides (NO_x) and can strongly affect tropospheric ozone distributions by transporting NO_x from the point of emission to remote locations. Furthermore PAN is known to be a secondary pollutant like ozone with negative impacts on regional air quality and human health (Dalsøren et al., 2018; Fischer et al., 2014; González Abad et al., 2011; Kort et al., 2016; Monks et al., 2018; Pozzer et al., 2020; Rudolph, 1995; Tzompa-Sosa et al., 2017).

Several recent studies have estimated global ethane budgets using a combination of observations and model simulations. Xiao et al. (2008) estimated a global ethane source of 13.0 Tg/yr based on methane emissions for the 1990s. This study included information on sectoral and geographical ethane emissions, although the inventory might partially be outdated, at least for North America, due to the changes in oil and gas extraction since 2004 (Tzompa-Sosa et al., 2017). Simpson et al. (2012) reported a total 21% decrease in global ethane emissions from 14.3 to 11.3 Tg/yr from 1984 to 2010, likely due to the decline in fugitive emissions from fossil fuel extraction and use. Monks et al. (2018) estimated the global ethane emission in 2008 to be 15.4 ± 2.3 Tg/yr. Hausmann et al. (2016) calculated the contribution from oil and natural gas to the total ethane emission increase of 1-11 Tg/yr over 2007-2014. Franco et al. (2016) reported a global ethane emission of 18.2 Tg/yr for 2014 and that North American anthropogenic ethane emissions increased by 75% over 2008-2014. Helmig et al. (2016) calculated a growth rate 0.42 (0.19) Tg/yr of NH ethane emission



between mid-2009 and mid-2014, and Pozzer et al. (2020) estimated a 2.1 Tg/yr increase of global anthropogenic ethane from 13.2 to 15.3 Tg/yr over the same period.

60 Despite the general agreement in global emission estimates, multiple studies have pointed out that the current inventories used in atmospheric chemistry models underestimate ethane emissions by up to a factor of 2-3 (Angot et al., 2021; Dalsøren et al., 2018; Emmons et al., 2015; Franco et al., 2016; Monks et al., 2018; Pétron et al., 2014; Tilmes et al., 2016; Tzompa-Sosa et al., 2017). Dalsøren et al. (2018) concluded that the major source of uncertainty in these inventories comes from the assumed speciation of NMVOCs (non-methane volatile organic compounds) and
65 disaggregation of carbon emissions into individual species based on little available data. Therefore, in order to determine the global ethane trend with greater certainty, long-term global ethane datasets with minimal local influences are required (Angot et al., 2021; Gardiner et al., 2008).

Previous studies attempting to understand the distribution, emissions, lifetime, and atmospheric trends of ethane have tended to be from surface sites, either from a regionally focused intensive
70 field measurement campaign (e.g. Kort et al. (2016)) or from networks of remote sampling stations (e.g. Franco et al. (2015), Helmig et al. (2016)). The advantage of surface sites is that they are easily accessed and maintained, however, such measurements inevitably reflect the local or regional situation and changes in emissions immediately upwind of a measurement location can affect the results, masking any underlying long-term global trend. In addition, most ethane
75 measurement sites are located in developed countries, such as in North America and Europe, while ethane observations in the rest of the world are sparse. This too hinders the assessment of global ethane trends, for while one country's emission may be declining another's could be increasing rapidly. For the aforementioned reasons it is advantageous to assess the global long-term ethane trend from the upper troposphere and even the stratosphere where emissions can be
80 expected to be well mixed by atmospheric circulations. In particular the trend of ethane in the more isolated and remote stratosphere is of interest when assessing long-term changes.

In this study, we use airborne observations covering the Northern Hemisphere (NH), including over regions where ground measurements are not setup or not possible. We present long-term global and geographically delineated (North America, Asia, Europe) ethane trends in the upper
85 troposphere and stratosphere for the decade 2006-2016 derived using airborne measurements and global model simulations. In addition, the trends of methane and propane collected from the same



observations are examined to better understand the observed variation of NH ethane trends, as they have common sources and sinks in the atmosphere. All the data used in this study are publicly available at <https://doi.org/10.5281/zenodo.5112059>. These data can be used for further analysis on global and regional trends, emissions and lifetime of methane, ethane, and propane, their contributions to climate change, stratosphere-troposphere exchange, and improvement of current inventories and atmospheric models.

2. Materials and Methods

2.1 IAGOS-CARIBC observation

The IAGOS-CARIBIC project (In-service Aircraft for a Global Observing System-Civil Aircraft for the Regular Investigation of the atmosphere Based on an Instrument Container) is an aircraft based scientific project with the aim of monitoring long-term global atmospheric physics and chemistry (Brenninkmeijer et al., 2007). The flight altitudes are at ~10 km, which is in the Upper Troposphere-Lower Stratosphere (UTLS) region. A custom built whole air sampler collects pressurized air samples during each flight, and these samples are subsequently measured in the laboratory with Gas Chromatography (GC) coupled with three detectors: GC-ECD for greenhouse gas measurements (methane, carbon dioxide, nitrous oxide and sulphur hexafluoride) (Schuck et al., 2009), and GC-FID and GC-AED for volatile organic compound measurements, including ethane and propane (Baker et al., 2010; Karu et al., 2021). The precision of ethane and propane data used in this study is 0.2% and 0.8%, respectively (Baker et al., 2010), and of methane 0.17% (Schuck et al., 2009). Details regarding measurement procedure, calibration scales are well documented in the cited references.

2.2 EMAC global model

The ECHAM/MESSy Atmospheric Chemistry (EMAC) model is a numerical chemistry and climate simulation system that includes sub-models describing tropospheric and middle atmosphere processes and their interaction with oceans, land and human influences (Jöckel et al.,



2010). It uses the second version of the Modular Earth Submodel System (MESSy2) to link multi-
115 institutional computer codes. The core atmospheric model is the 5th generation European Centre
Hamburg general circulation model (ECHAM5, Roeckner et al. (2006)). For the present study we
applied EMAC (ECHAM5 version 5.3.02, MESSy version 2.55.0) in the T63L47MA-resolution,
i.e. with a spherical truncation of T63 (corresponding to a quadratic Gaussian grid of approx. 1.8
by 1.8 degrees in latitude and longitude) with 47 vertical hybrid pressure levels up to 0.01 hPa (~80
120 km). The model has been weakly nudged towards the ERA5 reanalysis data of the ECMWF
(Hersbach et al., 2020). The chemical mechanism comprises methane, alkanes and alkenes up to
C₄, ozone, odd nitrogen, some selected non-methane hydrocarbons (NMHCs), heterogeneous
reactions, etc. In total, 310 reactions of 155 species are included in the model. The photolysis rates
are calculated following Sander et al. (2014). No chlorine chemistry is included in the model. To
125 account for realistic emissions, the CAMS-GLOB-ANT v4.2 emission inventory data is used for
model simulations (Granier et al., 2019; Guevara et al., 2020).

It has been shown by multiple studies that the ethane emissions due to fossil fuel combustion are
strongly underestimated in the emissions database (Guevara et al., 2021; Helmig et al., 2016;
Pozzer et al., 2020). In this work, we therefore increased the anthropogenic emissions of ethane of
130 a factor of 2.47 to match (for the year 2010) the total amount suggested by Pozzer et al. (2020)
although this value slightly underestimates the measured concentration as shown in Pozzer et al.
(2020). In the later sections of this paper, we further increased the total emission by 45% to match
the airborne observation data, and the estimated ethane emissions from natural and anthropogenic
sources are presented in Table 1, together with description for each sector and optimized sectoral
135 emissions (will be discussed in the *Results and Discussion* section).

In this study, two types of ethane trends were presented with the model simulation: (1) constant
meteorology and constant emission (hereafter called climatology), sampled at the IAGOS-
CARIBIC sampling location with S4D algorithm (sampling in 4 dimensions) described in Jöckel
et al. (2010). Any trends (or changes) detected in this simulation would be caused by differences
140 in sample location and timing. (2) real meteorological conditions from ECMWF and the adjusted
emissions described above, sampled at the IAGOS-CARIBIC sampling location with S4D
algorithm (Jöckel et al., 2010).



2.3 Trend analysis

The trend and seasonality analysis algorithm (“Prophet”) used in this study has been described in
145 detail elsewhere (Taylor and Letham, 2018). The “Prophet” algorithm has been shown to perform
well with non-continuous time series datasets (Li et al., 2021a), as is the case for the aircraft data.
The trend analysis model has four components: trend (non-periodic changes), seasonality (periodic
changes), holiday effects, and error (idiosyncratic changes). In this study, effects of holidays are
not included. We used a linear model with change points for the trend component, and the trend
150 function consists of growth rate, adjustments of growth rate and offset parameter. The flexibility
of trend (e.g. overfitting or underfitting) can be adjusted by the parameter
“changepoint_prior_scale”. Seasonality is estimated by Fourier series (Harvey and Shephard,
1993). The uncertainty interval was set to be 95%. The code of trend analysis in Python for this
study can be found in the Supplementary Material. Figure S1 shows the ethane trend and
155 seasonality at Iceland estimated by “Prophet” algorithm. Compared with the trend and seasonality
estimated by NOAA algorithm (www.esrl.noaa.gov/gmd/ccgg/mbl/crvfit/crvfit.html) using the
same dataset in Figure 1(b) of Helmig et al. (2016), the seasonality of ethane is well captured by
both algorithms and the results match well with each other. The uncertainty from the trend analysis
is estimated by applying ten fitting levels on the trend (i.e. “changepoint_prior_scale” = 0.1, 0.2,
160 0.3, ..., 0.9, 1.0). The difference between the most underfitting to most overfitting is taken as the
uncertainty and the average value of the ten fitting levels is used to represent the underlying long-
term trend.

3. Results and Discussion

165 3.1 Literature perspective of global ethane trends

Many studies have reported ethane trend analysis based on either ground-based sampling or FTIR
(Fourier Transform Infrared Spectrometer) measurements. A summary of these studies is shown in
Table 2. In the troposphere (Table 2(a)), the trends of C₂H₆ partial column at four European sites
(Jungfraujoch, Zugspitze, Harestua and Kiruna) during 1996-2006 were between about -1.09 to -
170 2.11%/yr (Angelbratt et al., 2011). Simpson et al. (2012) concluded a strong global ethane decline



of 21% over 26 years (1984-2010), with a stronger decline occurring from 1984 to 1999 (-7.2 ± 1.7 ppt/yr) than from 2000 to 2010 (-1.9 ± 1.3 ppt/yr). Franco et al. (2015) showed the ethane trend at Jungfraujoch to be $-0.92\%/yr$ during 1994-2008, followed by a strong positive trend of $4.9\%/yr$ during 2009-2014, which may be related to the growth of shale gas exploitation in North America.

175 Helmig et al. (2016) calculated a mean ethane growth rate of $2.9-4.7\%/yr$ from 2009 to 2014 at 32 NH ground measurement sites, and concluded that North American oil and gas development was the primary source of the increasing emission of ethane. Franco et al. (2016) compared the ethane total column change at six sites across NH for the period of 2003-2008 and 2009-2014, and also revealed a sharp increase of $3-5\%/yr$ during 2009-2014 compared with 2003-2008, which was

180 associated with oil and gas industry emission. They also specifically estimated a 1.2 Tg/yr increase of anthropogenic ethane emission from North America between 2008-2014. Hausmann et al. (2016) presented a positive ethane trend of ca. $4.6\%/yr$ at Zugspitze (47° N) and a negative trend of ca. $-2.5\%/yr$ at Lauder (45° S) for 2007-2014, and inferred an ethane increase from oil and gas emission of $1-11$ Tg/yr for 2007-2014. Angot et al. (2021) showed an increase in ethane trend of ca. $5.6\%/yr$

185 at GEOSummit (73° N) for 2010-2014, followed by a temporary pause of ethane growth in 2015-2018. Sun et al. (2021) presented a negative ethane trend of $-2.6 \pm 1.3\%/yr$ over 2015-2020 in a densely populated eastern Chinese city Hefei. In this study, we estimated an increasing NH upper tropospheric ethane trend of $0.33 \pm 0.27\%/yr$ (mean \pm 1SD) between February 2006 and February 2016.

190 In contrast to tropospheric ethane trends, trends in the stratosphere have been far less investigated. Gardiner et al. (2008) (Table 2 (b)) presented annual trend in stratospheric ethane column (relative to year 2000) at six sites and these varied from 0.43 to $-3.31\%/yr$ until the year 2005. Franco et al. (2015) reported ethane trends at $8-16$ km measured at Jungfraujoch of $-1.75 \pm 1.30\%/yr$ (for 2004-2008) and $9.4 \pm 3.2\%/yr$ (for 2009-2013), indicating an $\sim 11\%$ sharp increase since 2009. Helmig

195 et al. (2016) showed that the UTLS column ethane ($8-21$ km) measured at Jungfraujoch was decreasing at $-1.0 \pm 0.2\%/yr$ (1995-2009) and started a sharp increase at rate of $6.0 \pm 1.1\%/yr$ from 2009 until 2015, while the difference in trend growth rate between the two time periods is smaller for the mid-tropospheric column ($3.6-8$ km): $-0.8 \pm 0.3\%/yr$ (1995-2009) and $4.2 \pm 1.0\%/yr$ (2009-2015). In this study, we derived a NH lowermost stratospheric ethane decreasing trend of $-3.6 \pm$

200 $0.3\%/yr$ for the period February 2006 – February 2016.



3.2 Overview of IAGOS-CARIBC observations

In total 6,607 Northern Hemispheric samples were collected during Feb 2006-Feb 2016. 51% of them (3,365 samples) are identified as upper tropospheric samples ($PV < 2$), the rest 49% (3,242) samples are stratospheric samples. All samples are categorized into four groups based on their sampling locations: North America (NAM), Asia (ASI), Europe (EUR) and Rest of the world (ROW) (Table S1). Temporal and spatial distributions of sample number are shown in Figure S2.

The observed upper tropospheric ethane concentration shows clear seasonality (Figure 1) driven by the atmospheric hydroxyl radical (OH) cycle and emissions. Upper tropospheric NAM and EUR ethane concentrations increase from October/November peaking in April, decreases from April until October. This is consistent with the FTIR observation (Franco et al., 2015). Upper tropospheric ASI ethane peaks in June, two months later than NAM and EUR, and has two smaller peaks in October and February. In contrast, the stratospheric ethane concentration does not show any clear seasonality, except that NAM has a seasonal trend with 3-month later shift compared to the upper tropospheric NAM trend.

3.3 Tropospheric trends

3.3.1 Upper tropospheric observation vs. model simulation

Figure 2 shows the upper tropospheric ethane trends and corresponding uncertainties (Figure S3 (a)) from the observations, the model and model optimizations (section 2.2), the top 5 contributing model sectors, and the climatology.

As the air samples were not collected in exactly the same positions (e.g. altitude, latitude, longitude), the observed trends of trace gases could be potentially influenced by biases between the sampling locations. The trends presented in this study represent those from a selected number of observations. In order to assess whether a sampling location bias is associated with the derived trend, the measured trends were compared to results from a global model (EMAC) where the modeled data were extracted at the nearest grid of latitude, longitude, altitude and time to the



original measurement. Figure 2 (a) (grey line) shows the upper tropospheric ethane trend from the EMAC simulation with constant meteorology and constant year-to-year emission with seasonal cycle (climatology). Thus if a trend is indicated from the model data, then it is expected to be associated with the sampling location rather than a real underlying trend. Although small variations of the ethane trend are observed due to the sampling location, these are negligible compared to the trend derived from the observations, implying that the different spatio-temporal sampling locations did not influence the estimated trends.

We then focus on the ethane trends in the whole NH upper troposphere, and in addition, three regions: NAM, EUR and ASI, whose emissions are estimated to be the dominant sources of global ethane emissions, accounting for 58~63% in 2008 (Monks et al., 2018). A clear increasing trend in ethane between Feb 2006-May 2010 of 19.2%/yr (± 4.8 , 1SD) relative to Feb 2006 and a decreasing trend in May 2010-Feb 2016 of 7.5%/yr (± 1.1) relative to May 2010 were observed for the upper troposphere (Figure 2 (a)). Such trend patterns are observed for all three regions of interest (NAM, ASI, EUR in Figure 2 (b)(c)(d)). Interestingly they are the inverse of the trends observed at the surface stations: a decreasing trend before 2009 and a sharp increase in 2009-2014 (Franco et al., 2015; Franco et al., 2016; Helmig et al., 2016; Simpson et al., 2012). To understand the driving factors behind the observed trends, we simulated the ethane concentration with the atmospheric model (EMAC) for the IAGOS-CARIBIC samples (see section 2.2).

The trends from the model simulations and the optimized model results (increasing the input model emissions by 45%) are shown in Figure 2 as red and blue lines. The initial model results underestimate ethane concentration by about 45%, whereas the performance is much better with the same model and observation dataset for the simulation of methane (Zimmermann et al., 2020). The model incorporates all known emissions via emission inventories so any deviations between model and measurements can be interpreted as indicators of hitherto unknown emissions or sinks, atmospheric processes or errors in emission inventories. The optimized model results match reasonably well with the measured NH upper tropospheric trend (Figure 2 (a)). However, this is not the case for the regional scales. A significant discrepancy between model and observation for NAM and ASI appears in 2010-2011 (Figure 2 (b)(c)). As the model includes fixed emissions or emissions with prescribed changes, such an abrupt increase in the ethane trend for NAM and ASI in 2010-2011 is presumably due to a short-term additional source that generated a large-scale



ethane plume. A likely source is the Deepwater Horizon oil spill in 2010 that released 0.64 billion
liters oil into the Gulf of Mexico followed by a global transport of ethane to other continents
260 (Camilli et al., 2010; Ryerson et al., 2011; Unified Command Deepwater Horizon, 2010). The
model simulates an inverse trend compared to the observed trend for EUR (Figure 2 (d)), although
CAM5-GLOB-ANT dataset has already included emission inventories for some major European
cities (Guevara et al., 2021).

The top 5 contributing model sectors for ethane source trends are FEF (fugitives), RES (residential
265 energy use), TRO (road transportation), SWD (solid waste and waste water) and BIB (biomass
burning), and their optimized trends are shown in Figure 2. The pronounced peak in 2010-2011 for
the NH upper tropospheric ethane is related to the increase in FEF, RES and SWD, and the
decreasing trend in 2011-2013 can be explained by the decrease in FEF, RES and BIB (Figure 2
(a)). SWD and TRO contributed most for the trends in NAM, ASI and EUR, while FEF, BIB and
270 RES have similar contribution (Figure 2 (b)(c)(d)).

Figure 3 shows the sectoral contribution to regional and global ethane trends. The width of flow is
proportional to the quantity of sectoral contribution. Our model results estimated the average
contribution of biogenic (BIO), biomass burning (BIB) and anthropogenic sources (sum of all other
sectors) to the NH upper tropospheric ethane in 2006-2016 are 9%, 16%, and 75%, respectively.
275 This matches the estimated ~4%, 18%, and 78%, respectively, from Helmig et al. (2016). The
contribution of the top anthropogenic sources to upper tropospheric ethane are TRO (28.7%), SWD
(21.7%), FEF (14.0%), RES (6.0%), AWB (1.7%), and ENE (1.1%). Detailed relative
contributions of each sector are shown in Table S2. The contribution of TRO from this study is
more than that of ~10% estimated by Peischl et al. (2013); Warneke et al. (2012); Wunch et al.
280 (2016).

3.3.2 Model geographical sector contribution

Five geographical sectors, i.e. ASI, NAM, EUR, ROW and AIR+BIB+BIO (as they cannot be
separated into regions), were included to investigate the origin of the ethane emissions (Figure 4,
285 Figure S4). Ethane emission from ASI dominates the trends for the whole NH upper troposphere,
NAM, ASI and EUR, contributing 30%~55%, 35%~50%, 50%~65%, and 30%~40%, respectively.



Ethane emissions from ROW and AIR+BIB+BIO contribute 10%~25% each to the overall ethane trends. Emissions from EUR and NAM are the least contributors with each only 5%~20% contribution to ethane trends.

290 **3.3.3 Ethane, methane and propane trend comparison**

Methane and propane share emission sources with ethane, including fossil fuel extraction, transport and use, especially related to oil and natural gas (Bourtsoukidis et al., 2020; Dalsøren et al., 2018; Helmig et al., 2016; Zimmermann et al., 2020). Further, these three compounds share the same major sink in the atmosphere: oxidation by OH radical.

295 In 2006-2016, NH upper tropospheric ethane has a total change of 18.1 (mean) [min, max: -27.2, 29.4] ppt from observation, that corresponds to a change rate of 1.81 [-2.72, 2.94] ppt/yr, and 0.33 [-0.45, 0.55]%/yr relative to 2006. The observed NH upper tropospheric methane increases in total 63.2 [62.7, 63.6] ppb, corresponding to a growth rate of 6.32 [6.27, 6.36] ppb/yr (3.52 [3.49, 3.55] %/yr relative to 2006). In the same period, the observed NH upper tropospheric propane increases in
300 total 7.0 [-7.3, 11.1] ppt, representing a growth rate of 0.70 [-0.73, 1.11] ppt/yr (1.02 [-0.82, 1.72]%/yr relative to 2006).

For the whole NH upper troposphere, ethane and propane have similar trends in 2006-2016 (i.e. a rise and then a fall), whilst the observed methane trend follows an increase throughout that period (Figure 5). A common peak of all three compounds appears in 2010-2011, which possibly indicates
305 an abrupt increase in oil and gas emissions. This peak is also observed for ASI, EUR and NAM (not for NAM methane) (Figures S5, S6, S7), suggesting regional and global increase in fossil fuel emissions. The contribution of OH radical variation to the peak in 2010-2011 is expected to be small as several previous studies have shown the atmospheric OH concentration did not change significantly in that period (IPCC, 2013; Li et al., 2018; Montzka et al., 2011; Rigby et al., 2017).

310 NAM ethane and propane trends from the middle of 2014 to 2016 show a clear decline, probably due to a slowdown in U.S. natural gas emissions (Angot et al., 2021).



3.3.4 Model simulation for ground stations

Observations of surface ethane mixing ratios at two ground stations (Mauna Loa (MLO), and
315 Hohenpeissenberg (HPB)) were compared with model simulations using the optimized emissions
from this study. The model predicts the ethane at the surface well, for both stations in NAM and
EUR. This confirms that the optimized ethane emission budget derived from the upper
tropospheric and stratospheric observation is realistic for surface-level ethane too.

3.3.5 Ethane emission budget

The global ethane emission budget was estimated to be 19.28 Tg/yr for February 2006 to February
2016, with biogenic emissions 0.78 Tg/yr, biomass burning 1.46 Tg/yr and anthropogenic
emissions 17.05 Tg/yr (Table 1). This budget matches well with the estimated ethane emissions
from other studies, e.g. 18.2 Tg/yr for 2014 from Franco et al. (2016) and somewhat higher than
325 the 15.3 Tg/yr (anthropogenic emission) for 2014 from Pozzer et al. (2020).

3.4 Stratospheric trends

3.4.1 Observation vs. model simulation

While ground based stations will be affected by upwind sources, the stratospheric samples offer a
330 remote and averaged global perspective. Stratospheric ethane trends, estimated with all the IAGOS-
CARIBIC samples taken in the NH lowermost stratosphere with potential velocity (PV) larger than
2 PVU during 2006-2016, along with modeled stratospheric trends, are shown in Figure 6
(corresponding uncertainties in Figure S3 (b)). The stratospheric climatology (Figure 6 (a)) varies
more than the tropospheric one, but it is again minor contribution for observed trends, so that
335 location biased trends can be discounted. The observed stratospheric ethane shows a general trend
of $-3.6 (\pm 0.3)\%/yr$ in 2006-2016, with two exceptional peaks in 2010 and 2013. The peak in 2010
is not seen at regional levels (NAM, ASI, EUR, Figure 6 (b)(c)(d)), which would have indicated
global upward transport of the upper tropospheric ethane emissions (peaking in 2010-2011) into
the stratosphere. The second peak in 2013 is assumed to be due to the regional emission transport
340 into the lowermost stratosphere as such a peak is observed simultaneously over NAM and ASI. In



general, the optimized model trend matches well with the observed NH stratospheric trend in 2006-2013 (Figure 6 (a)). A noticeable discrepancy between the optimized model simulation and observation appears since 2013. In the stratosphere, the OH radical concentration on average decreases by a factor of 10 compared with tropospheric OH levels, whereas Cl radicals are more abundant and therefore plays a greater relative role in ethane oxidation (Li et al., 2018). The chlorine chemistry is not included in our model but the abundance of chlorine in the stratosphere is a significant loss factor for ethane, thus part of the observed discrepancy can come from the missing chlorine chemistry in the model. After 2013, the model prediction for ASI was far from observation (Figure 6(c)), but this was not the case for other regions. This could also explain the larger discrepancy between model and observation since 2013.

The top 5 contributing model sectors for stratospheric ethane trends, at global and regional scales, are TRO (~28%), SWD (~24%), BIB (~15%), FEF (~13%), and RES (7%) (Figure 3, Table S2), their optimized trends are shown in Figure 6.

Model geographical sector contributions for the stratospheric ethane trends are shown in Figure 7 and Figure S8. Similar to the upper troposphere, ASI ethane emissions contribute the most to the global and regional stratospheric ethane trends (~45%). We attribute this to the Asian Monsoon transport of air pollutants from the troposphere to the stratosphere, which is supported by other studies (Bian et al., 2020; Lelieveld et al., 2002; Lelieveld et al., 2018; Park et al., 2009; Randel et al., 2010). Ethane emissions from ROW and AIR+BIB+BIO contribute 15-20% each, and EUR and NAM 10-15% each.

3.4.2 Ethane, methane and propane trend comparison

Figure 8 shows the observed stratospheric trends of ethane, methane, and propane in 2006-2016. The observed NH stratospheric ethane has a total change of -191.3 [-221.2, -166.7] ppt corresponding to a change rate of -19.13 [-22.12, -16.67] ppt/yr, and -3.59 [-4.15, 3.20]/yr relative to 2006. The observed methane in the NH stratosphere increases in total 36.9 [34.5, 38.0] ppb, that represents a growth rate of 3.69 [3.45, 3.80] ppb/yr (2.09 [1.95, 2.15] %/yr) relative to 2006. In the same period, the observed NH stratospheric propane declined in total 52.2 [51.3, 55.7] ppt, that corresponds to a decline rate of 5.22 [5.13, 5.57] ppt/yr (5.58 [5.45, 6.09]/yr) relative to



370 2006. The regional trends of ethane, propane and methane at NAM, ASI and EUR are shown in Figures S9, S10, and S11.

Similar to the upper tropospheric trends, ethane and propane shared similar trends in the NH stratosphere, NAM and EUR. The 2010-2011 peak observed in the upper troposphere also appears in the stratosphere, indicating a strong influence of troposphere-stratosphere exchange. It is noted
375 that the observed stratospheric trends on regional scales represent a mixture of local emission and global atmospheric transport.

4. Data availability

The IAGOS-CARIBIC observational data of ethane, methane, and propane in the period February
380 2006 – February 2016, and optimized ethane mixing ratios in sectors from EMAC model simulation for the same IAGOS-CARIBIC samples and time period, can be accessed at <https://doi.org/10.5281/zenodo.5112059> (Li et al., 2021b). Co-authorship may be appropriate if the data are essential for a result or conclusion of a publication.

385 5. Conclusions

In this study, we present upper tropospheric and lower stratospheric ethane trends from airborne observations and atmospheric modeling over the period 2006-2016. The model performance was optimized by scaling to the observational data. We identified ethane sectoral sources to which observed average trends over ten years (2006-2016) and three continents (North America,
390 Europe, and Asia) could be attributed from observation and modeling. Trends of ethane, propane and methane from observation were compared to identify ethane emission sources. The major findings are summarized as follows:

- The global ethane emission budget for February 2006 to February 2016 was estimated to be 19.28 Tg/yr. In the Northern Hemisphere, the upper tropospheric ethane had an
395 increasing trend of $0.33 \pm 0.27\%/yr$ and the stratospheric ethane had a decreasing trend of



-3.6 ± 0.3%/yr for 2006-2016. The current inventory underestimates ethane emission by roughly a factor of three.

- The top five contributing model sectors for upper tropospheric and stratospheric ethane trends are FEF (fugitives), RES (residential energy use), TRO (road transportation), SWD (solid waste and waste water) and BIB (biomass burning). Emissions from Asia dominate the observed ethane trends for both upper troposphere and lower stratosphere.
- A sharp increase in the observed upper tropospheric and stratospheric ethane trends at global and regional scales in 2010-2011 was caused by fossil fuel related emissions, likely from oil associated and natural gas sources. In contrast to methane, the global ethane trends cannot be well simulated by advanced atmospheric chemistry modeling, which suggests the need of accurate and frequent observations of global ethane and the improvement of emission inventories.

Author contribution

M.L. and J.W. developed the idea of this study. M.L. wrote the first draft of the manuscript. A.P. run the model simulations. All authors contributed to discuss and revise the manuscript.

Competing interests

The authors declare no conflict of interests.

415

Acknowledgement

We are thankful to Sourangsu Chowdhury for preparing the model emission input data into different regions, and Nils Noll for providing biomass burning emission budget for ethane. We thank Tobias Sattler for contributing to the initial idea of this study. We thank NOAA for sharing ground station data of ethane.

420



References

- 425 Angelbratt, J., Mellqvist, J., Simpson, D., Jonson, J. E., Blumenstock, T., Borsdorff, T., Duchatelet, P., Forster, F., Hase, F., Mahieu, E., De Mazière, M., Notholt, J., Petersen, A. K., Raffalski, U., Servais, C., Sussmann, R., Warneke, T., and Vigouroux, C.: Carbon monoxide (CO) and ethane (C₂H₆) trends from ground-based solar FTIR measurements at six European stations, comparison and sensitivity analysis with the EMEP model, *Atmos. Chem. Phys.*, 11, 9253-9269, 2011.
- 430 Angot, H., Davel, C., Wiedinmyer, C., Pétron, G., Chopra, J., Hueber, J., Blanchard, B., Bourgeois, I., Vimont, I., Montzka, S. A., Miller, B. R., Elkins, J. W., and Helmig, D.: Temporary pause in the growth of atmospheric ethane and propane in 2015–2018, *Atmos. Chem. Phys. Discuss.*, 2021, 1-34, 2021.
- Baker, A. K., Slemr, F., and Brenninkmeijer, C. A. M.: Analysis of non-methane hydrocarbons in air samples collected aboard the CARIBIC passenger aircraft, *Atmos. Meas. Tech.*, 3, 311-321, 2010.
- 435 Bian, J., Li, D., Bai, Z., Li, Q., Lyu, D., and Zhou, X.: Transport of Asian surface pollutants to the global stratosphere from the Tibetan Plateau region during the Asian summer monsoon, *National Science Review*, 7, 516-533, 2020.
- 440 Bourtsoukidis, E., Pozzer, A., Sattler, T., Matthaios, V. N., Ernle, L., Edtbauer, A., Fischer, H., Könemann, T., Osipov, S., Paris, J. D., Pfannerstill, E. Y., Stöner, C., Tadic, I., Walter, D., Wang, N., Lelieveld, J., and Williams, J.: The Red Sea Deep Water is a potent source of atmospheric ethane and propane, *Nature Communications*, 11, 447, 2020.
- 445 Brenninkmeijer, C. A. M., Crutzen, P., Boumard, F., Dauer, T., Dix, B., Ebinghaus, R., Filippi, D., Fischer, H., Franke, H., Frief, U., Heintzenberg, J., Helleis, F., Hermann, M., Kock, H. H., Koepfel, C., Lelieveld, J., Leuenberger, M., Martinsson, B. G., Miemczyk, S., Moret, H. P., Nguyen, H. N., Nyfeler, P., Oram, D., O'Sullivan, D., Penkett, S., Platt, U., Pucek, M., Ramonet, M., Randa, B., Reichelt, M., Rhee, T. S., Rohwer, J., Rosenfeld, K., Scharffe, D., Schlager, H., Schumann, U., Slemr, F., Sprung, D., Stock, P., Thaler, R., Valentino, F., van Velthoven, P., Waibel, A., Wandel, A., Waschitschek, K., Wiedensohler, A., Xueref-Remy, I., Zahn, A., Zech, U., and Ziereis, H.: Civil Aircraft for the regular investigation of the atmosphere based on an instrumented container: The new CARIBIC system, *Atmos. Chem. Phys.*, 7, 4953-4976, 2007.
- 450 Camilli, R., Reddy, C. M., Yoerger, D. R., Van Mooy, B. A. S., Jakuba, M. V., Kinsey, J. C., McIntyre, C. P., Sylva, S. P., and Maloney, J. V.: Tracking Hydrocarbon Plume Transport and Biodegradation at Deepwater Horizon, *Science*, 330, 201, 2010.
- 455 Dalsøren, S. B., Myhre, G., Hodnebrog, Ø., Myhre, C. L., Stohl, A., Pisso, I., Schwietzke, S., Höglund-Isaksson, L., Helmig, D., Reimann, S., Sauvage, S., Schmidbauer, N., Read, K. A., Carpenter, L. J., Lewis, A. C., Punjabi, S., and Wallasch, M.: Discrepancy between simulated and observed ethane and propane levels explained by underestimated fossil emissions, *Nature Geoscience*, 11, 178-184, 2018.
- 460 Emmons, L. K., Arnold, S. R., Monks, S. A., Huijnen, V., Tilmes, S., Law, K. S., Thomas, J. L., Raut, J. C., Bouarar, I., Turquety, S., Long, Y., Duncan, B., Steenrod, S., Strode, S., Flemming, J., Mao, J., Langner, J., Thompson, A. M., Tarasick, D., Apel, E. C., Blake, D. R., Cohen, R. C., Dibb, J., Diskin, G. S., Fried, A., Hall, S. R., Huey, L. G., Weinheimer, A. J., Wisthaler, A., Mikoviny, T., Nowak, J., Peischl, J., Roberts, J. M., Ryerson, T., Warneke, C., and Helmig, D.: The POLARCAT Model Intercomparison Project (POLMIP): overview and evaluation with observations, *Atmos. Chem. Phys.*, 15, 6721-6744, 2015.
- Fischer, E. V., Jacob, D. J., Yantosca, R. M., Sulprizio, M. P., Millet, D. B., Mao, J., Paulot, F., Singh, H. B., Roiger, A., Ries, L., Talbot, R. W., Dzepina, K., and Pandey Deolal, S.: Atmospheric peroxyacetyl nitrate (PAN): a global budget and source attribution, *Atmos. Chem. Phys.*, 14, 2679-2698, 2014.
- 465 Franco, B., Bader, W., Toon, G. C., Bray, C., Perrin, A., Fischer, E. V., Sudo, K., Boone, C. D., Bovy, B., Lejeune, B., Servais, C., and Mahieu, E.: Retrieval of ethane from ground-based FTIR solar spectra using improved spectroscopy: Recent burden increase above Jungfraujoch, *Journal of Quantitative Spectroscopy and Radiative Transfer*, 160, 36-49, 2015.
- 470 Franco, B., Mahieu, E., Emmons, L. K., Tzompa-Sosa, Z. A., Fischer, E. V., Sudo, K., Bovy, B., Conway, S., Griffin, D., Hannigan, J. W., Strong, K., and Walker, K. A.: Evaluating ethane and methane emissions associated



- with the development of oil and natural gas extraction in North America, *Environmental Research Letters*, 11, 044010, 2016.
- 475 Gardiner, T., Forbes, A., de Mazière, M., Vigouroux, C., Mahieu, E., Demoulin, P., Velazco, V., Notholt, J., Blumenstock, T., Hase, F., Kramer, I., Sussmann, R., Stremme, W., Mellqvist, J., Strandberg, A., Ellingsen, K., and Gauss, M.: Trend analysis of greenhouse gases over Europe measured by a network of ground-based remote FTIR instruments, *Atmos. Chem. Phys.*, 8, 6719-6727, 2008.
- 480 González Abad, G., Allen, N. D. C., Bernath, P. F., Boone, C. D., McLeod, S. D., Manney, G. L., Toon, G. C., Carouge, C., Wang, Y., Wu, S., Barkley, M. P., Palmer, P. I., Xiao, Y., and Fu, T. M.: Ethane, ethyne and carbon monoxide concentrations in the upper troposphere and lower stratosphere from ACE and GEOS-Chem: a comparison study, *Atmospheric Chemistry and Physics*, 11, 9927-9941, 2011.
- 485 Granier, C., Darras, S., van der Gon, H. D., Jana, D., Elguindi, N., Bo, G., Michael, G., Marc, G., Jalkanen, J.-P., and Kuenen, J.: The Copernicus Atmosphere Monitoring Service global and regional emissions (April 2019 version), 2019. 2019.
- 490 Guevara, M., Jorba, O., Tena, C., Denier van der Gon, H., Kuenen, J., Elguindi-Solmon, N., Darras, S., Granier, C., and Pérez García-Pando, C.: CAMS-TEMPO: global and European emission temporal profile maps for atmospheric chemistry modelling, *Earth Syst. Sci. Data*, 2021, 1-60, 2020.
- Guevara, M., Jorba, O., Tena, C., Denier van der Gon, H., Kuenen, J., Elguindi, N., Darras, S., Granier, C., and Pérez García-Pando, C.: Copernicus Atmosphere Monitoring Service TEMPORal profiles (CAMS-TEMPO): global and European emission temporal profile maps for atmospheric chemistry modelling, *Earth Syst. Sci. Data*, 13, 367-404, 2021.
- Harvey, A. C. and Shephard, N.: 10 Structural time series models, 1993. 1993.
- Hausmann, P., Sussmann, R., and Smale, D.: Contribution of oil and natural gas production to renewed increase in atmospheric methane (2007–2014): top–down estimate from ethane and methane column observations, *Atmos. Chem. Phys.*, 16, 3227-3244, 2016.
- 495 Helmig, D., Rossabi, S., Hueber, J., Tans, P., Montzka, S. A., Masarie, K., Thoning, K., Plass-Duelmer, C., Claude, A., Carpenter, L. J., Lewis, A. C., Punjabi, S., Reimann, S., Vollmer, M. K., Steinbrecher, R., Hannigan, J. W., Emmons, L. K., Mahieu, E., Franco, B., Smale, D., and Pozzer, A.: Reversal of global atmospheric ethane and propane trends largely due to US oil and natural gas production, *Nature Geoscience*, 9, 490-495, 2016.
- 500 Hersbach, H., Bell, B., Berrisford, P., Hirahara, S., Horányi, A., Muñoz-Sabater, J., Nicolas, J., Peubey, C., Radu, R., Schepers, D., Simmons, A., Soci, C., Abdalla, S., Abellan, X., Balsamo, G., Bechtold, P., Biavati, G., Bidlot, J., Bonavita, M., De Chiara, G., Dahlgren, P., Dee, D., Diamantakis, M., Dragani, R., Flemming, J., Forbes, R., Fuentes, M., Geer, A., Haimberger, L., Healy, S., Hogan, R. J., Hólm, E., Janisková, M., Keeley, S., Laloyaux, P., Lopez, P., Lupu, C., Radnoti, G., de Rosnay, P., Rozum, I., Vamborg, F., Villaume, S., and Thépaut, J.-N.: The ERA5 global reanalysis, *Quarterly Journal of the Royal Meteorological Society*, 146, 1999-2049, 2020.
- 505 IPCC: Climate change 2013: the physical science basis: Working Group I contribution to the Fifth assessment report of the Intergovernmental Panel on Climate Change, edited by: Stocker, T. F., Qin, D., Plattner, G.-K., Tignor, M., Allen, S. K., Boschung, J., Nauels, A., Xia, Y., Bex, V., and Midgley, P. M, Cambridge university press, 2013.
- Jöckel, P., Kerkweg, A., Pozzer, A., Sander, R., Tost, H., Riede, H., Baumgaertner, A., Gromov, S., and Kern, B.: Development cycle 2 of the Modular Earth Submodel System (MESSy2), *Geosci. Model Dev.*, 3, 717-752, 2010.
- 510 Karu, E., Li, M., Ernle, L., Brenninkmeijer, C. A., Lelieveld, J., and Williams, J.: Atomic emission detector with gas chromatographic separation and cryogenic pre-concentration (CryoTrap-GC-AED) for trace gas measurement, *Atmospheric Measurement Techniques*, doi: 10.5194/amt-2020-199, 2021. 2021.
- Kort, E. A., Smith, M. L., Murray, L. T., Gvakharia, A., Brandt, A. R., Peischl, J., Ryerson, T. B., Sweeney, C., and Travis, K.: Fugitive emissions from the Bakken shale illustrate role of shale production in global ethane shift, *Geophysical Research Letters*, 43, 4617-4623, 2016.
- Lelieveld, J., Berresheim, H., Borrmann, S., Crutzen, P., Dentener, F., Fischer, H., Feichter, J., Flatau, P., Heland, J., and Holzinger, R.: Global air pollution crossroads over the Mediterranean, *Science*, 298, 794-799, 2002.
- Lelieveld, J., Bourtsoukidis, E., Brühl, C., Fischer, H., Fuchs, H., Harder, H., Hofzumahaus, A., Holland, F., Marno, D., and Neumaier, M.: The South Asian monsoon—pollution pump and purifier, *Science*, 361, 270-273, 2018.



- 520 Li, M., Karu, E., Brenninkmeijer, C., Fischer, H., Lelieveld, J., and Williams, J.: Tropospheric OH and stratospheric OH and Cl concentrations determined from CH₄, CH₃Cl, and SF₆ measurements, *Nature Climate and Atmospheric Science*, 1, 2018.
- Li, M., Karu, E., Ciais, P., Lelieveld, J., and Williams, J.: The empirically determined integrated atmospheric residence time of carbon dioxide (CO₂), in review, 2021a. 2021a.
- 525 Li, M., Pozzer, A., Lelieveld, J., and Williams, J.: Global atmospheric ethane, propane and methane trends (2006-2016) [*data set*]. Zenodo (<https://doi.org/10.5281/zenodo.5112059>) 2021b.
- Millet, D. B., Guenther, A., Siegel, D. A., Nelson, N. B., Singh, H. B., de Gouw, J. A., Warneke, C., Williams, J., Eerdeken, G., Sinha, V., Karl, T., Flocke, F., Apel, E., Riemer, D. D., Palmer, P. I., and Barkley, M.: Global atmospheric budget of acetaldehyde: 3-D model analysis and constraints from in-situ and satellite observations, *Atmos. Chem. Phys.*, 10, 3405-3425, 2010.
- 530 Monks, S. A., Wilson, C., Emmons, L. K., Hannigan, J. W., Helmig, D., Blake, N. J., and Blake, D. R.: Using an Inverse Model to Reconcile Differences in Simulated and Observed Global Ethane Concentrations and Trends Between 2008 and 2014, *Journal of Geophysical Research: Atmospheres*, 123, 11,262-211,282, 2018.
- 535 Montzka, S. A., Krol, M., Dlugokencky, E., Hall, B., Jockel, P., and Lelieveld, J.: Small interannual variability of global atmospheric hydroxyl, *Science*, 331, 67-69, 2011.
- Park, M., Randel, W. J., Emmons, L. K., and Livesey, N. J.: Transport pathways of carbon monoxide in the Asian summer monsoon diagnosed from Model of Ozone and Related Tracers (MOZART), *Journal of Geophysical Research: Atmospheres*, 114, 2009.
- 540 Peischl, J., Ryerson, T. B., Brioude, J., Aikin, K. C., Andrews, A. E., Atlas, E., Blake, D., Daube, B. C., de Gouw, J. A., Dlugokencky, E., Frost, G. J., Gentner, D. R., Gilman, J. B., Goldstein, A. H., Harley, R. A., Holloway, J. S., Kofler, J., Kuster, W. C., Lang, P. M., Novelli, P. C., Santoni, G. W., Trainer, M., Wofsy, S. C., and Parrish, D. D.: Quantifying sources of methane using light alkanes in the Los Angeles basin, California, *Journal of Geophysical Research: Atmospheres*, 118, 4974-4990, 2013.
- 545 Pétron, G., Karion, A., Sweeney, C., Miller, B. R., Montzka, S. A., Frost, G. J., Trainer, M., Tans, P., Andrews, A., Kofler, J., Helmig, D., Guenther, D., Dlugokencky, E., Lang, P., Newberger, T., Wolter, S., Hall, B., Novelli, P., Brewer, A., Conley, S., Hardesty, M., Banta, R., White, A., Noone, D., Wolfe, D., and Schnell, R.: A new look at methane and nonmethane hydrocarbon emissions from oil and natural gas operations in the Colorado Denver-Julesburg Basin, *Journal of Geophysical Research: Atmospheres*, 119, 6836-6852, 2014.
- 550 Pozzer, A., Schultz, M. G., and Helmig, D.: Impact of U.S. Oil and Natural Gas Emission Increases on Surface Ozone Is Most Pronounced in the Central United States, *Environmental Science & Technology*, 54, 12423-12433, 2020.
- Randel, W. J., Park, M., Emmons, L., Kinnison, D., Bernath, P., Walker, K. A., Boone, C., and Pumphrey, H.: Asian monsoon transport of pollution to the stratosphere, *Science*, 328, 611-613, 2010.
- 555 Rigby, M., Montzka, S. A., Prinn, R. G., White, J. W. C., Young, D., O'Doherty, S., Lunt, M. F., Ganesan, A. L., Manning, A. J., Simmonds, P. G., Salameh, P. K., Harth, C. M., Muhle, J., Weiss, R. F., Fraser, P. J., Steele, L. P., Krummel, P. B., McCulloch, A., and Park, S.: Role of atmospheric oxidation in recent methane growth, *Proc Natl Acad Sci U S A*, 114, 5373-5377, 2017.
- Roeckner, E., Brokopf, R., Esch, M., Giorgetta, M., Hagemann, S., Kornblueh, L., Manzini, E., Schlese, U., and Schulzweida, U.: Sensitivity of Simulated Climate to Horizontal and Vertical Resolution in the ECHAM5 Atmosphere Model, *Journal of Climate*, 19, 3771-3791, 2006.
- 560 Rudolph, J.: The tropospheric distribution and budget of ethane, *Journal of Geophysical Research: Atmospheres*, 100, 11369-11381, 1995.
- Ryerson, T. B., Aikin, K. C., Angevine, W. M., Atlas, E. L., Blake, D. R., Brock, C. A., Fehsenfeld, F. C., Gao, R. S., de Gouw, J. A., Fahey, D. W., Holloway, J. S., Lack, D. A., Lueb, R. A., Meinardi, S., Middlebrook, A. M., Murphy, D. M., Neuman, J. A., Nowak, J. B., Parrish, D. D., Peischl, J., Perring, A. E., Follack, I. B., Ravishankara, A. R., Roberts, J. M., Schwarz, J. P., Spackman, J. R., Stark, H., Warneke, C., and Watts, L. A.: Atmospheric emissions from the Deepwater Horizon spill constrain air-water partitioning, hydrocarbon fate, and leak rate, *Geophysical Research Letters*, 38, 2011.



- 570 Sander, R., Jöckel, P., Kirner, O., Kunert, A. T., Landgraf, J., and Pozzer, A.: The photolysis module JVAL-14, compatible with the MESSy standard, and the JVal PreProcessor (JVPP), *Geosci. Model Dev.*, 7, 2653-2662, 2014.
- Schuck, T. J., Brenninkmeijer, C. A. M., Slemr, F., Xueref-Remy, I., and Zahn, A.: Greenhouse gas analysis of air samples collected onboard the CARIBIC passenger aircraft, *Atmos. Meas. Tech.*, 2, 449-464, 2009.
- 575 Simpson, I. J., Sulbaek Andersen, M. P., Meinardi, S., Bruhwiler, L., Blake, N. J., Helmig, D., Rowland, F. S., and Blake, D. R.: Long-term decline of global atmospheric ethane concentrations and implications for methane, *Nature*, 488, 490-494, 2012.
- Sun, Y., Yin, H., Liu, C., Mahieu, E., Notholt, J., Té, Y., Lu, X., Palm, M., Wang, W., Shan, C., Hu, Q., Qin, M., Tian, Y., and Zheng, B.: Reduction in C₂H₆ from 2015 to 2020 over Hefei, eastern China points to air quality improvement in China, *Atmos. Chem. Phys. Discuss.*, 2021, 1-29, 2021.
- Taylor, S. J. and Letham, B.: Forecasting at scale, *The American Statistician*, 72, 37-45, 2018.
- 580 Tilmes, S., Lamarque, J. F., Emmons, L. K., Kinnison, D. E., Marsh, D., Garcia, R. R., Smith, A. K., Neely, R. R., Conley, A., Vitt, F., Val Martin, M., Tanimoto, H., Simpson, I., Blake, D. R., and Blake, N.: Representation of the Community Earth System Model (CESM1) CAM4-chem within the Chemistry-Climate Model Initiative (CCMI), *Geosci. Model Dev.*, 9, 1853-1890, 2016.
- 585 Tzompa-Sosa, Z. A., Mahieu, E., Franco, B., Keller, C. A., Turner, A. J., Helmig, D., Fried, A., Richter, D., Weibring, P., Walega, J., Yacovitch, T. I., Herndon, S. C., Blake, D. R., Hase, F., Hannigan, J. W., Conway, S., Strong, K., Schneider, M., and Fischer, E. V.: Revisiting global fossil fuel and biofuel emissions of ethane, *Journal of Geophysical Research: Atmospheres*, 122, 2493-2512, 2017.
- Unified Command Deepwater Horizon: US scientific teams refine estimates of oil flow from BP's well prior to capping, *Gulf of Mexico Oil Spill Response 2010*, 2010. 2010.
- 590 Warneke, C., de Gouw, J. A., Holloway, J. S., Peischl, J., Ryerson, T. B., Atlas, E., Blake, D., Trainer, M., and Parrish, D. D.: Multiyear trends in volatile organic compounds in Los Angeles, California: Five decades of decreasing emissions, *Journal of Geophysical Research: Atmospheres*, 117, 2012.
- 595 Wunch, D., Toon, G. C., Hedelius, J. K., Vizenor, N., Roehl, C. M., Saad, K. M., Blavier, J.-F. L., Blake, D. R., and Wennberg, P. O.: Quantifying the loss of processed natural gas within California's South Coast Air Basin using long-term measurements of ethane and methane, *Atmospheric Chemistry and Physics*, 16, 14091-14105, 2016.
- Xiao, Y., Logan, J. A., Jacob, D. J., Hudman, R. C., Yantosca, R., and Blake, D. R.: Global budget of ethane and regional constraints on U.S. sources, *Journal of Geophysical Research: Atmospheres*, 113, 2008.
- 600 Zimmermann, P. H., Brenninkmeijer, C. A. M., Pozzer, A., Jöckel, P., Winterstein, F., Zahn, A., Houweling, S., and Lelieveld, J.: Model simulations of atmospheric methane (1997–2016) and their evaluation using NOAA and AGAGE surface and IAGOS-CARIBIC aircraft observations, *Atmos. Chem. Phys.*, 20, 5787-5809, 2020.



Figures and Tables

605 Table 1. Sectoral description and ethane emissions estimated from this study for Feb 2006-Feb 2016.

Sector	Description	Emission (Tg/yr)
BIO	Biogenic emission	0.78
BIB	Biomass burning	1.46
(a) Anthropogenic by sector		
AWB	Agricultural waste burning	0.12
	Power generation (power and heat plants, refineries, others)	0.06
ENE		
FEF	Fugitives	7.65
IND	Industrial processes	1.30
RES	Residential energy use	4.82
SHP	Ships	0.03
SLV	Solvents	0.00
SWD	Solid waste and waste water	1.47
TNR	Off-road transportation	0.02
TRO	Road transportation	1.59
(b) Anthropogenic by geographical sector		
ASI	Emission from Asia	7.48
EUR	Emission from Europe	2.32
NAM	Emission from North America	1.46
ROW	Emission from rest of the world	5.79
Total source		19.28



Table 2. Summary of studies reporting ethane trends in the (a) troposphere and (b) stratosphere.

Trends (%/year)	Time period	References
(a) Tropospheric trends		
-1.09 ~ -2.11 (four European sites)	1996-2006	Angelbratt et al. (2011)
-0.81 (global)	1986-2010	Simpson et al. (2012)
-0.92 (Jungfrauoch, 47° N)	1994-2008	Franco et al. (2015)
4.9 (Jungfrauoch, 47° N)	2009-2014	Franco et al. (2015)
2.9-4.7 (32 ground sites)	2009-2014	Helmig et al. (2016)
3-5 (six sites)	2009-2014	Franco et al. (2016)
	compared with 2003-2008	
ca. 4.6 (Zugspitze, 47° N)	2007-2014	Hausmann et al. (2016)
ca. -2.5 (Lauder, 45° S)	2007-2014	Hausmann et al. (2016)
ca. 5.6 (GEOSummit, 73° N)	01.2010-12.2014	Angot et al. (2021)
-2.6 ± 1.34 (Hefei, 32° N)	2015-2020	Sun et al. (2021)
0.33 ± 0.27 (Northern Hemispheric upper troposphere)	02.2006-02.2016	This study
(b) Stratospheric trends		
-3.31 ~ 0.43 (stratospheric column)	2000-2005	Gardiner et al. (2008)
-1.75 ± 1.30 (8-16km above Jungfrauoch)	2004-2008	Franco et al. (2015)
-1.0 ± 0.2 (8-21km above Jungfrauoch)	1995-2009	Helmig et al. (2016)
9.4 ± 3.2 (8-16km above Jungfrauoch)	2009-2013	Franco et al. (2015)
6.0 ± 1.1 (8-21km above Jungfrauoch)	2009-2015	Helmig et al. (2016)
-3.6 ± 0.3 (Northern Hemispheric lowermost stratosphere)	02.2006-02.2016	This study

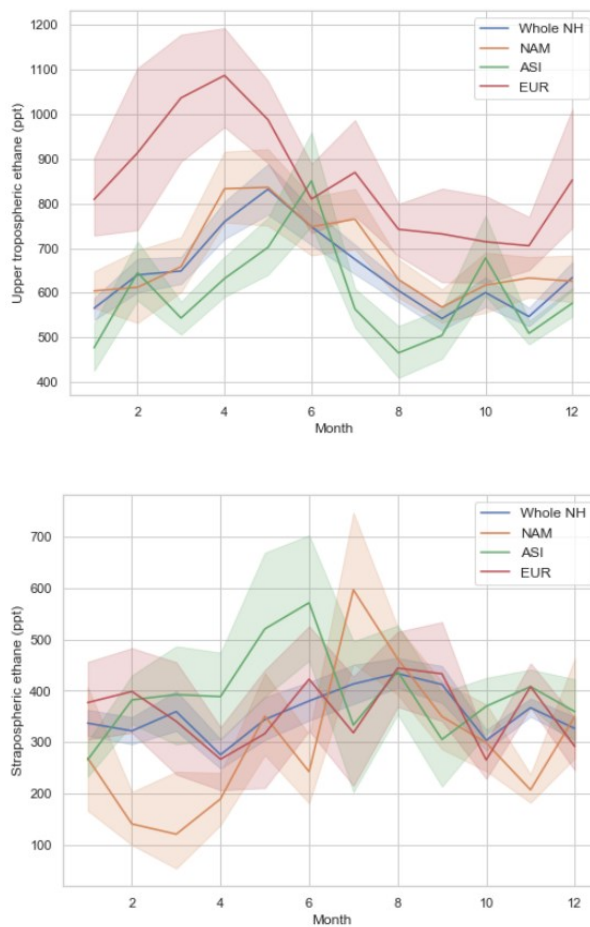


Figure 1. Seasonality of upper tropospheric and stratospheric ethane concentrations.

615

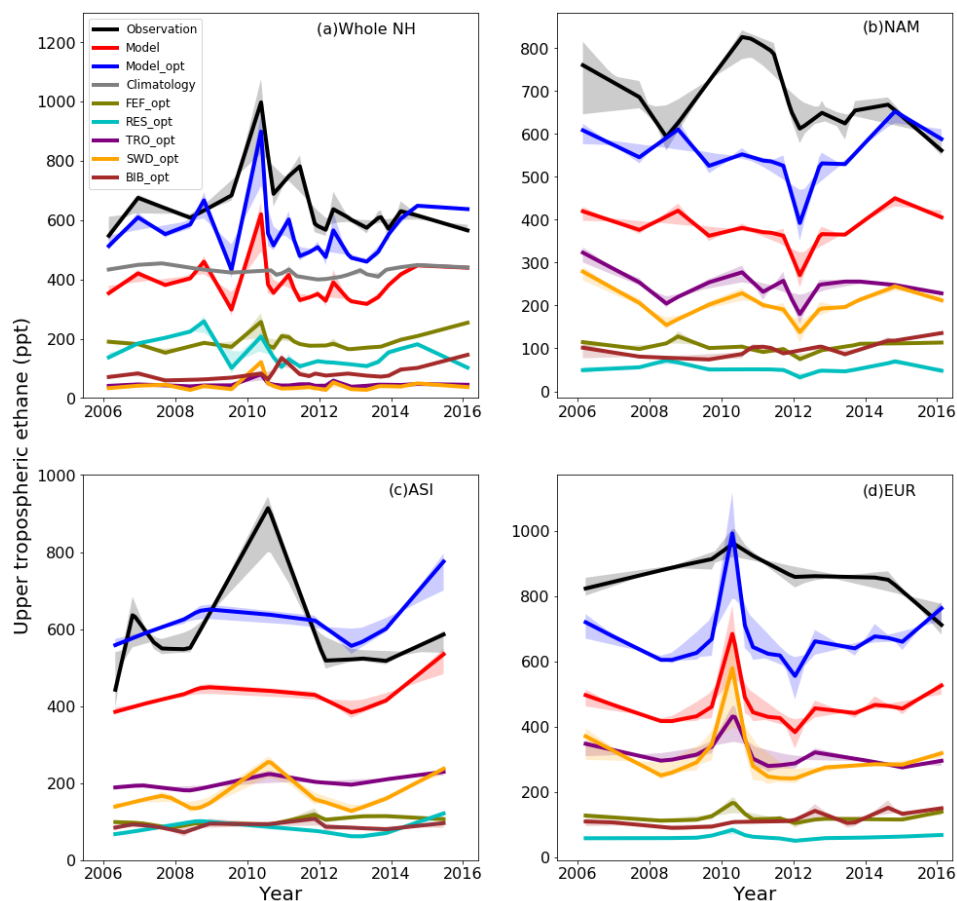
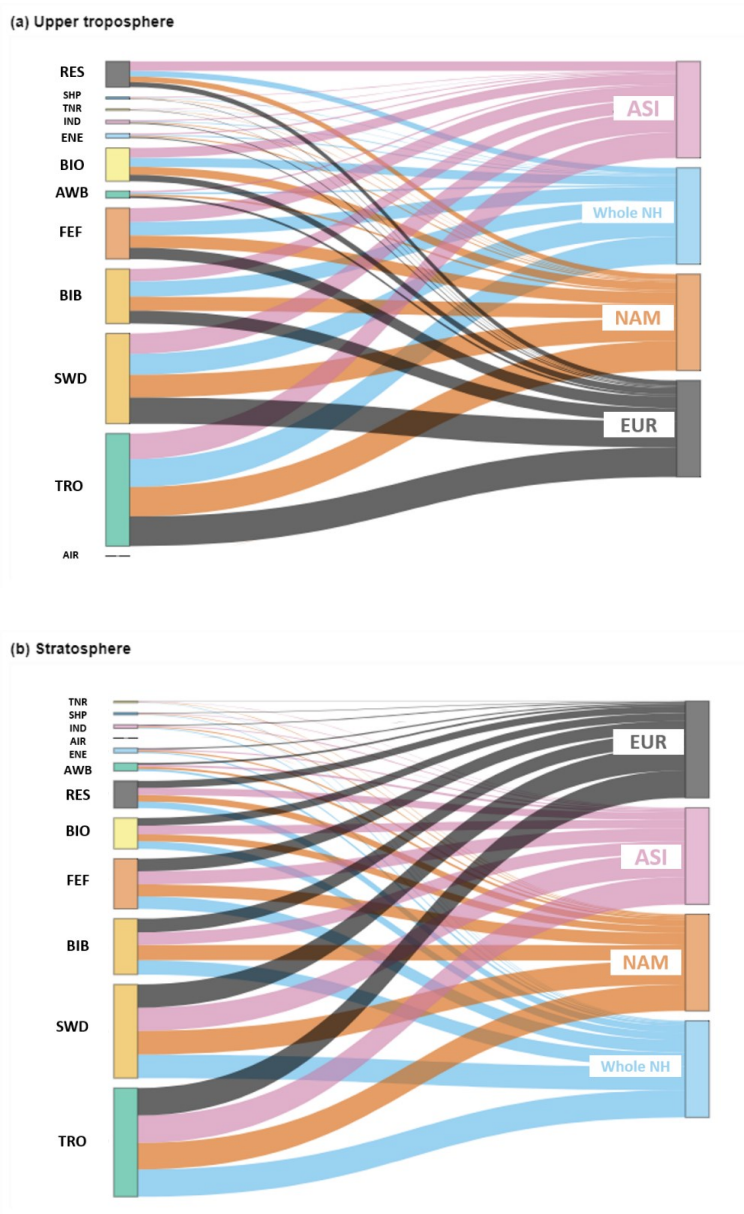


Figure 2. Upper tropospheric ethane trends from observations, the model and model optimization for (a) the whole NH; (b) North America; (c) Asia; and (d) Europe. Light shadows indicate trend analysis uncertainty.

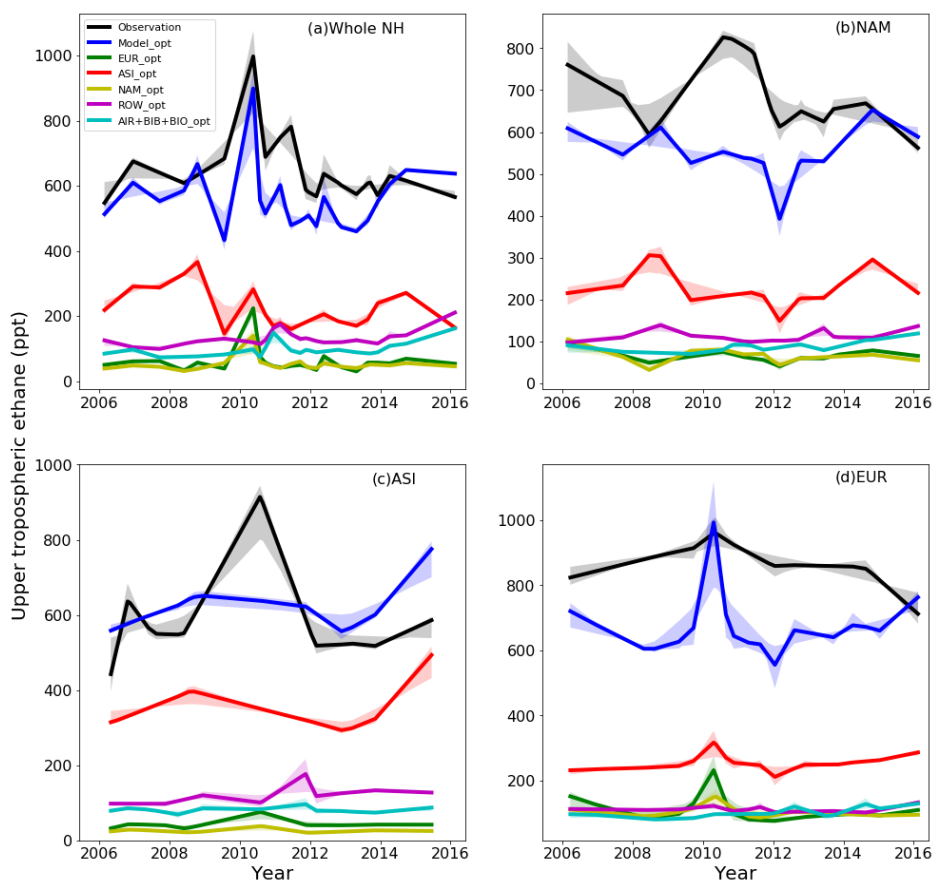


625

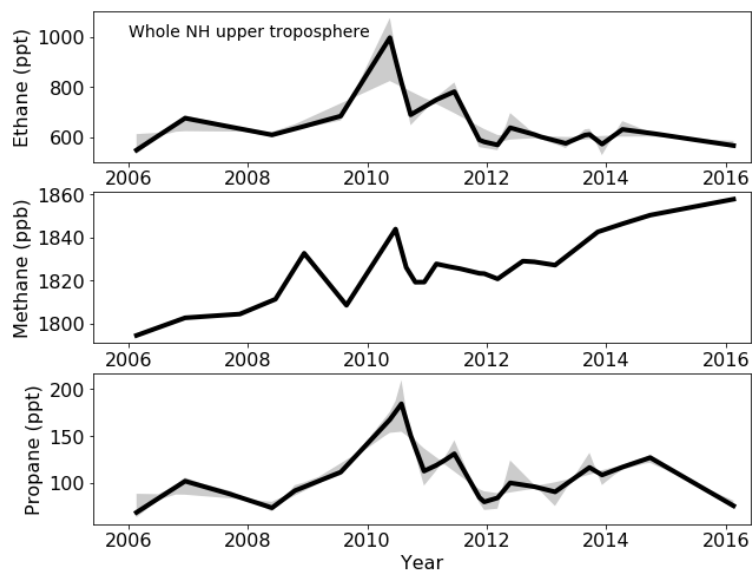
Figure 3. Sectoral contribution to ethane trends for the (a) upper troposphere and (b) stratosphere in 2006-2016.



630



635 Figure 4. Optimized geographical sector contribution (emissions from EUR, ASI, NAM, and ROW) to NH upper tropospheric ethane trends for (a) the whole NH; (b) North America; (c) Asia; and (d) Europe. Light shadows indicate trend analysis uncertainty.



640

Figure 5. The observed (a) ethane; (b) methane; (c) propane trends for the whole NH upper troposphere. Light shadows indicate trend analysis uncertainty.



645

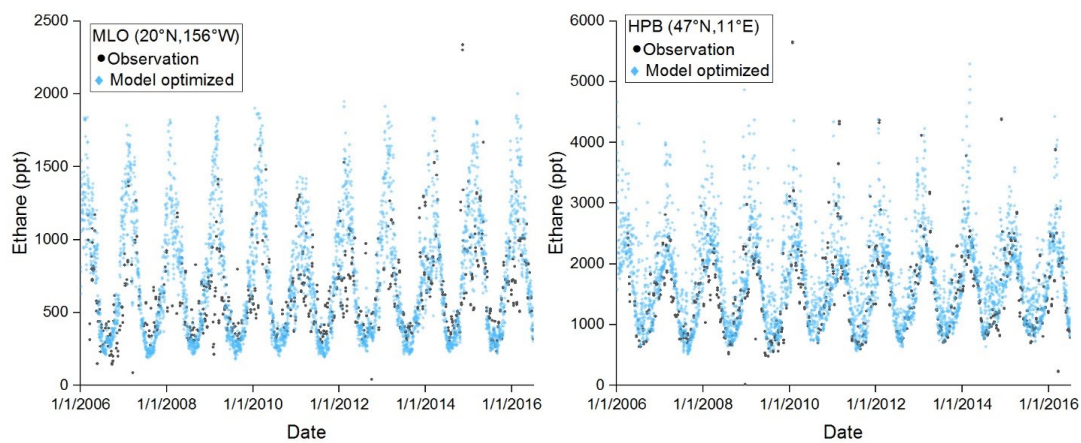
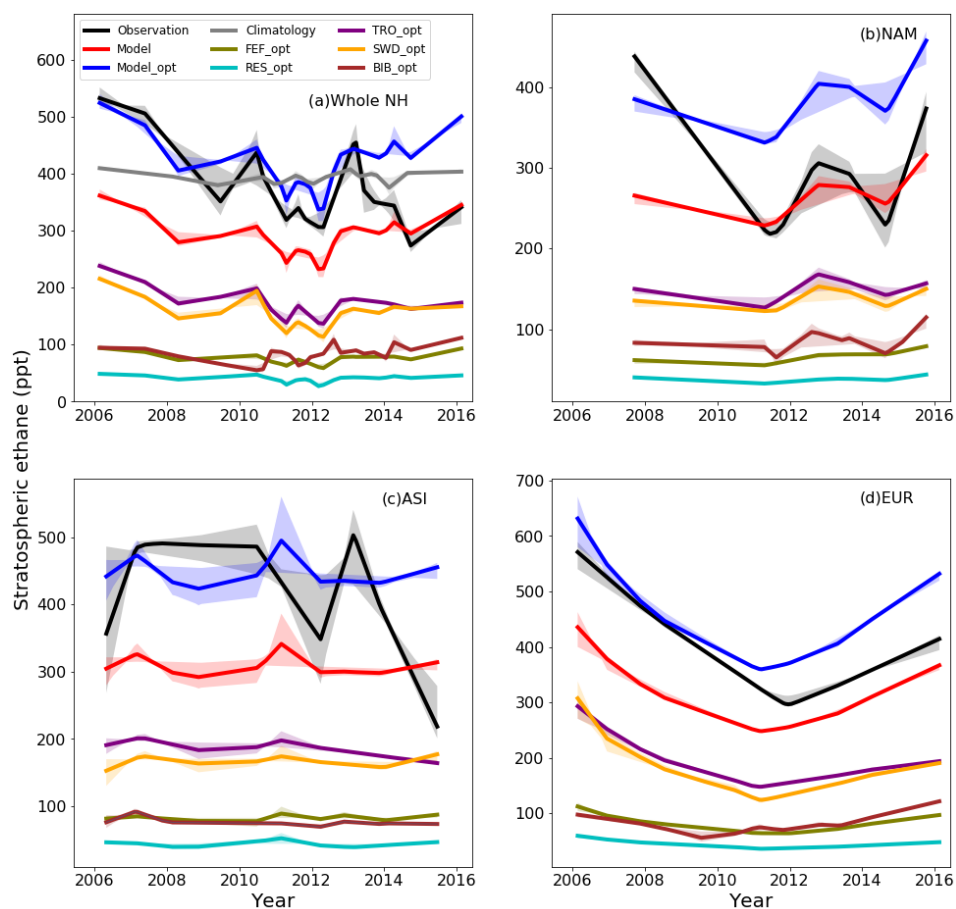


Figure 5. Observations and optimized model simulations for ethane mixing ratios at two ground stations (MLO, HPB).

650



655 Figure 6. Stratospheric ethane trends from observation, model and model optimization for (a) the whole NH stratosphere; (b) North America; (c) Asia; and (d) Europe. Light shadows indicate trend analysis uncertainty.



660

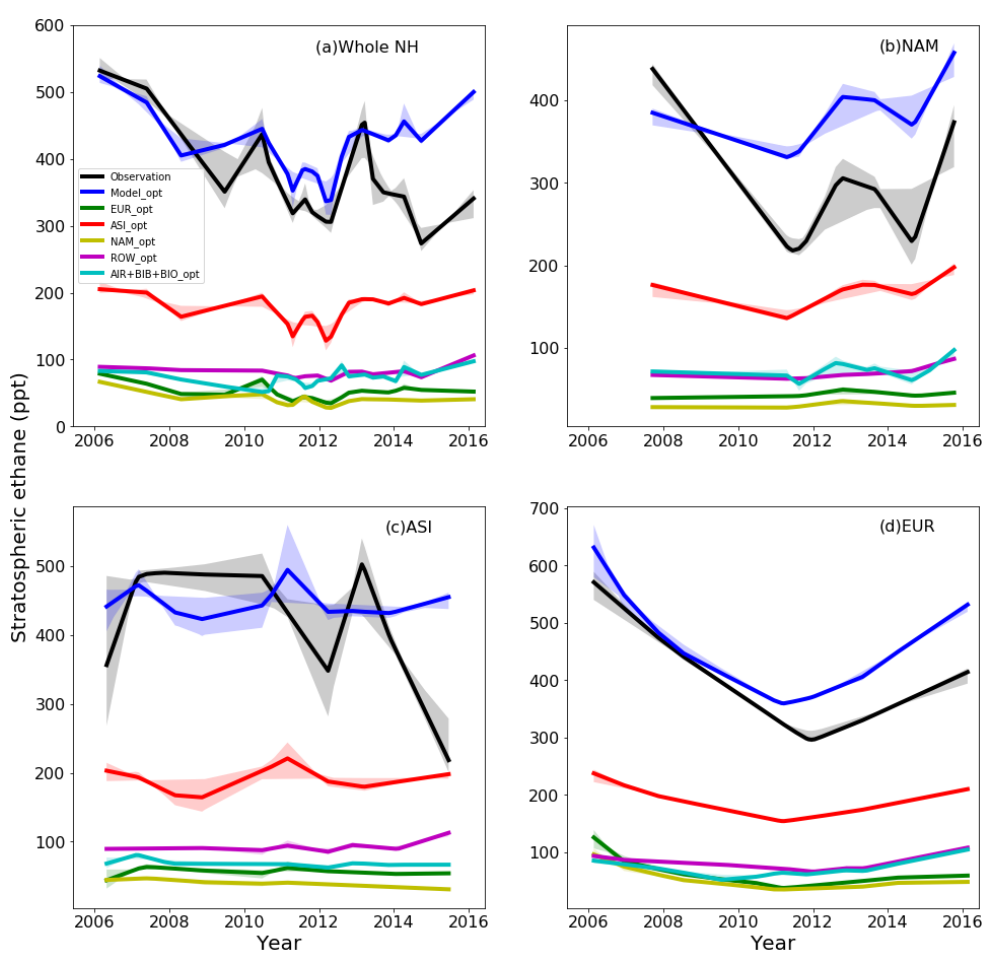
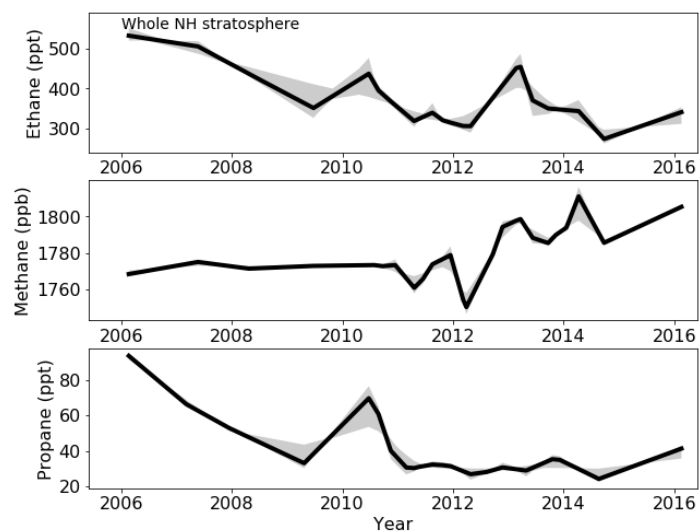


Figure 7. Optimized geographical sector contribution (emissions from EUR, ASI, NAM, and ROW) to stratospheric ethane trends for (a) the whole NH stratosphere; (b) North America; (c) Asia; and 665 (d) Europe. Light shadows indicate trend analysis uncertainty.



670

Figure 8. The observed (a) ethane; (b) methane; (c) propane trends for the whole NH stratosphere. Light shadows indicate trend analysis uncertainty.